The Use of Porous Media Models and CFD for Sulfur Treating Applications

Sean M. McGuffie, P.E.
Porter McGuffie, Inc.
Lawrence, KS, USA
sean@pm-engr.com

Dennis H. Martens, P.E.
Porter McGuffie, Inc.
Lawrence, KS, USA
martensdh@pm-engr.com

Michael A. Porter, P.E.
Porter McGuffie, Inc.
Lawrence, KS, USA
mike@pm-engr.com

Abstract:

Packed beds are used in numerous applications in sulfur recovery. During typical design processes, the flow through these beds is usually assumed to be uniformly distributed throughout the bed. Unfortunately, such is not always (or even mostly) the case. We will look at several different bed configurations and examine the flow conditions that typically exist and see what could be done to improve the flow.

In the first example, we see how a bed with non-uniform geometry can be modeled with a discrete particle geometric model to determine the porous media constants. Without sacrificing accuracy, the porous media model allows the analysis of large beds with much less computational overhead than models that include geometric complexity. In the second example, the analysis of a Tail Gas Unit (TGU) reactor will be demonstrated. This analysis will show how Computational Fluid Dynamics (CFD) can be used to analyze packed beds and as a design tool to optimize piping configurations. In this case the CFD analyses were able to make much more effective use of the catalyst bed, which has resulted in extended service life significantly reducing operating costs for the reactor. In the third example, a CFD analysis performed on an amine filter bed will demonstrate how the existence of more complicated features, such as bed voids, can be included to bracket the expected performance envelope of a bed. This example will also demonstrate the use of species wash-out tracking to determine the percent of bed utilization.

It is expected at the end of the presentation that conference attendees will understand the basics behind the incorporation of porous media models to model packed beds, their limitations, and how these models can be used to model their specific processes. While the accompanying paper will contain all theoretical details related to the porous media models, it is expected that the presentation will focus on examples, with the understanding that if attendees are interested in the “nuts and bolts” of the models that the paper will provide a solid framework to begin independent research.

1.0 Introduction:

Catalyst beds consist of an array of regular or irregular shaped particles randomly packed above a support structure. It is usual for the beds to consist of millions to tens of millions of particles. During the design of typical beds, the flow is usually assumed to be uniformly distributed with the bed pressure drop predicted through empirical methods such as the Ergun equation, or through physical testing of bed samples. While these methods have proven successful for adequate bed design, they have not achieved optimum bed designs as evidenced by bed bypass (indicated by reduced bed efficiency), bed scouring and shortened catalyst lives. To achieve a more optimal bed design, the designer can resort to two (2) methods, developing physical flow models, or developing computational models of the bed.

Physical flow models have previously been the primary choice for analysis of fluid dynamics. However, they are deficient in several areas:

- Cost,
- Similitude, and
- Flow visualization

Cost – Physical flow models are usually built to 1/10th to 1/12th scale, which can become large for some systems under consideration. They are typically one-off (i.e., built for each specific design) with very little reusability in components between even the most common designs. Specialized equipment is required to introduce and visualize the flow along with specialized personnel to conduct the testing. When all of these factors are considered, it is not uncommon for physical models along with testing of a system to cost over $100,000.

Similitude – Recall from basic fluid mechanics that most experimental fluid dynamics rely on the use of dimensional analysis to create dimensionless variables (Reynolds, Froude, Mach numbers, etc.) [1]. In physical testing a quantity known as similitude must be maintained. For physical models to predict the response of a full-scale system, certain ratios between the geometric and fluid property terms that make up the dimensionless numbers of relevance must be maintained (See Appendix – A, Theory). For simple systems such as the flow over aircraft or through ducts, it is relatively easy to maintain these ratios. Therefore, it can be stated that similitude is maintained and the performance of the physical model has relevance to the expected performance of the full-scale system when it is built.

In most cases, the difference in length scales in the system can require that similitude not be maintained. Consider the analysis of a process vessel with a packed bed. In this case the designer is likely interested in both the flow characteristics through the bulk of the vessel and through the bed. For these components there are two (2) disparate length scales, the characteristic length of the vessel and the characteristic length of the catalyst particles. This makes it impossible to write a consistent set of dimensionless equations to describe the entire system. In basic terms, to maintain the Reynolds number in the vessel, the Reynolds number for the catalyst particles will likely be orders of magnitude off. This is known in the model testing industry and requires development of models to focus on the variables related to the most important system components, usually related to the vessel. As you can see in this case, very little or any information could be gleaned relating to the exact flow patterns in the bed and their optimization.

Flow Visualization – While flow models are typically built from clear polycarbonate to allow views of the flow domain, it is known in the industry that there are limitations in the characterizations of the flow that can be achieved. In low-speed gaseous flows, it is typical to inject a tracer species to allow better visualization. While these tracers can be as elegant as the clean streamlines that occur during wind tunnel testing of cars and planes, the authors have also seen cases where puffs of smoke were injected into the flow, providing very little information about the actual flow patterns that were occurring. In any tracer test, the information that can be gathered is limited to where and what type of tracers can be injected. Additionally, all tests are limited by where visualization can be achieved in the model. Dark corners in the models, re-entrant corners and other typical design features do not lend themselves to ready visualization. Through careful design, arrays of probes can be placed in the test model that allow relatively detailed maps to be constructed of the flow field. These maps, however, are incomplete, only containing data at the probe points.

Additionally, there is uncertainty in the measured variables due to the probes' effect on the flow.

Computational fluid dynamics (CFD) models minimize or eliminate the three (3) drawbacks of physical models, as described above. The following points will address the advantages of CFD models, as compared to physical models.

Flow Visualization – CFD models allow the placement of any type of probe, the creation of any type of injector for tracer type evaluations and the use of cut planes to visualize or query any variable in the flow field. Additionally, the CFD model is not constrained by its physical placement in the test cell or where lights can be placed. Through simple mouse movements, the model and light sources can be rotated to view any point in the flow field. Additionally, the probes used in CFD models are virtual – they do not affect the flow field.

Similitude – All components in a CFD model are modeled at 1:1 scale to the equipment and the test fluid properties are the process properties that will occur in operation. Therefore, similitude is always achieved with a well-constructed CFD model. In fact, micron sized particle tracks can be considered in domains that contain hundreds of cubic feet without a problem.

Cost – As CFD models are virtual, equipment expense is saved in development and testing. Additionally, development of physical models requires highly skilled craftsman to build the model, highly trained technicians to oversee testing the model, and an experienced fluid dynamicist who will develop the model test plan, oversee the testing and interpret the results. Development and analysis of a CFD model only requires one or two experienced analysts. Due to these factors, it is now typically less expensive to conduct CFD analyses on reasonably sized models than to conduct physical testing. It should be noted that costs can increase exponentially for very large models (typically considered to be models larger than 20 – 30 million elements) due to the required computing facilities and the man-time required to create the models, monitor the solutions and post-process the results.

As can be seen from the comparison of physical and CFD models, CFD models are likely more advantageous than physical models for optimizing catalyst beds due to better flow visualization and the maintenance of similitude if costs can be constrained to be equivalent or less than physical models. It is obvious that CFD models that consider the entire catalyst bed in detail will be classified as very large models due to the number of catalyst particles and the requirements to model their geometry in detail. Therefore, to maintain a reasonable model size a simplification is usually used, a porous media model. This model does not model the individual catalyst particles; instead, using the procedures detailed in this paper, a simplification is made that allows full characterization of the bed's flow, without the computational overhead.

In addition to a brief description of the theoretical basis behind porous media models and how they are implemented in CFD software, this paper includes three industry examples to demonstrate the versatility of the porous media model for modeling many phenomena related to sulfur recovery.

1. Sample multi-layer catalyst bed – This example will consider a multi-

layered catalyst bed. In this case the basic procedures behind setting up the porous media models, including deriving the porous media constants both through the use of the Ergun equation and submodels is shown. The primary purpose of this example is to demonstrate the workflow and information required for a successful porous media analysis.

2. Tail gas unit (TGU) bed – This example will demonstrate how a CFD model that included a TGU catalyst bed was used to optimize the flow patterns in the vessel and its inlet piping to minimize pressure loss, and to optimize the flow into the catalyst bed. Included with this example is a demonstration of how modifications to the basic porous media model can be incorporated to allow prediction of the level of bed bypass caused by the reduced packing fraction in the near wall area.
3. Amine carbon filter bed – This example will expand upon the modifications demonstrated in the TGU analysis to show how additional model modifications can be incorporated to predict the decrease in bed performance caused by interstitial voids. The use of species tracers to provide direct measures of bed performance is demonstrated along with the porous media modifications required to consider the interstitial voids.

NOTE: While general discussion is provided for each example, the information contained in this paper should not be construed as design guidance. It should be recognized that each example is unique, necessitating detailed design based on the specific process conditions.

2.0 Porous Media, the Basis

In the simplest terms a porous media model is a model that represents the macroscopic flow effects of a porous structure, without modeling the microscopic flow details. This is achieved through a momentum sink term where lumped parameters are used to characterize the overall performance of the bed [2], computed as a pressure drop based on the superficial velocity. In any CFD software, a separate flow domain is created to model the overall packed bed space. The porous media model is applied to this domain.

Complete descriptions of the implementation of porous media models for three commercial CFD solvers, ANSYS-FLUENT, ANSYS-CFX and Star-CCM+ are shown in Appendix - A, Theory. As can be seen from the formulations given, the pressure drop through the porous media is dependent on the product of a constant and the velocity squared (the inertial term) and a second constant and the velocity (the viscous term). As will be shown later in this paper, in most cases these constants are easily determined.

Additional source or sink terms can also be incorporated in the porous media model to account for thermodynamic effects and/or chemical reactions. The inclusion of these terms is outside the scope of this paper.

3.0 Example 1 – Multi-layer Catalyst Bed

In the first example we will consider a generic catalyst bed to demonstrate how parameters for porous media models can be determined using two (2) methods, the

Ergun equation and through CFD submodels. The geometry and flow conditions for the bed under consideration were developed expressly for this example, based on past experience.

For this example, the catalyst bed sits at the bottom of an expansion section of a vessel. The bed consists of several layers of catalyst particles of various sizes supported on a hemispherical refractory structure. The hemispherical refractory structure has slots cut into the keys to allow flow through the slots. For this analysis of the catalyst bed, it is assumed that it is critical to verify that the flow is evenly distributed over the bed and that no recirculation occurs above the bed. Figure 1 shows the geometry of the model considered for this example. For simplification purposes it is assumed that the bed has three (3) layers of spherical particles (⌀ 0.75", 1.5" and 2") with perfect body-centered-cubic (BCC) packing. For the purpose of this paper, assume that the bed working fluid is air at STP (ρ = 1.18415 kg/m^3, $\mu = 1.86e^{-5}$ Pa-s). The void fraction is 0.42 for a perfect BCC packed bed.

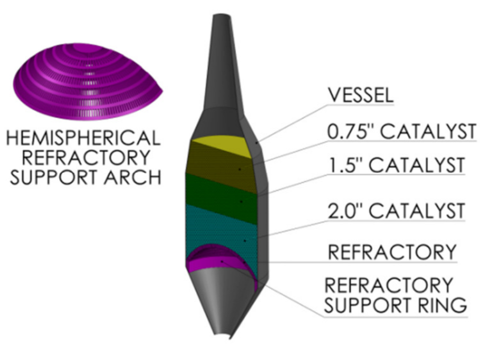

Figure 1 - Vessel Schematic for Mixing Region / Catalyst Bed Analysis

For this example procedures will be shown to complete the following tasks:

1. Determining the porous media parameters using the Ergun equation
2. Determining the porous media parameters using CFD submodels
3. Basic procedures to implement the multi-layer bed within CFD software, and
4. Basic procedures for validating the results of CFD analyses performed with porous media

3.1 Determination of Porous Media Parameters, Ergun Equation

Since the bed consists of spherical particles with a known packing fraction and a shape function of 1, the pressure drop as a function of bed depth can readily be predicted with the Ergun equation, as shown in Appendix A, Theory [6]. As can be seen from Equation 8 (from the Appendix), the Ergun equation consists of the sum of two terms. The term with linear dependence on velocity is the low Reynolds number (laminar) term, and the term with the dependence on velocity squared is the high Reynolds number (turbulent) term. Using this information, the pressure drop as a function of the bed depth and superficial velocity can be calculated and plotted for each catalyst particle diameter as shown in Figure 2.

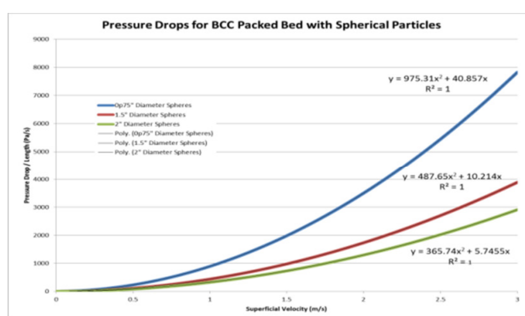

Figure 2 – Pressure Drops for Spherical Particles as Predicted by Ergun Equation

Also shown in the figure is that a second order fit, with a Y-intercept of zero (pressure drop at a 0 superficial velocity will always be 0), has been performed for each pressure drop series. The format for the pressure drop as a function of bed depth for Star-CCM+, is identical to the format of the fits shown in Figure 2, as shown in Appendix - A, Theory, Equation 7. In this case, the constants of the fits become the porous media model constants, the constant for the second order term becomes P_i and the first order term becomes P_v. To develop the constants for ANSYS-FLUENT or ANSYS-CFX, slight manipulation would be required. This would just involve modifying the polynomial fit terms to account for the viscosity and density of the fluid, as considered by the solver.

3.2 Determination of Porous Media Parameters, CFD Submodel

For simplicity's sake, the previous example was developed so that the Ergun equation was directly applicable, that the packing was perfect and even, and that there were no shape factors associated with the catalyst particles. It should be noted that it is possible to use CFD submodels to determine the constants required to implement the porous media model when the packing geometry does not lend itself to empirical modeling or when test data is not available, as shown in the continuation of this example.

To understand the steps involved in using CFD to determine the inputs required for a porous media model, consider the center bed in the previous case with 1.5" diameter spheres. In this case, a geometric model of the particles' packing can be constructed, as shown in Figure 3. Using common tools available in most CAD or CFD packages, such a packing structure can then be used to create a flow volume, or the void area between the particles where the fluid will flow. Figure 4 shows such a domain constructed for the packed bed represented in Figure 3. In this figure the peach colored walls are the domain extents, modeled with symmetry boundary conditions, and the light blue walls are the actual walls used to model the catalyst particles.

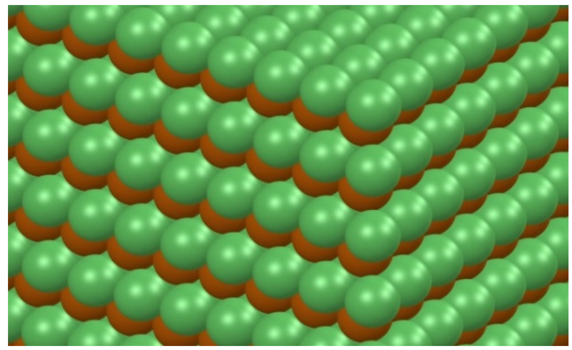

Figure 3 – Geometric Model for BCC Packed 1.5" Diameter Catalyst Spheres

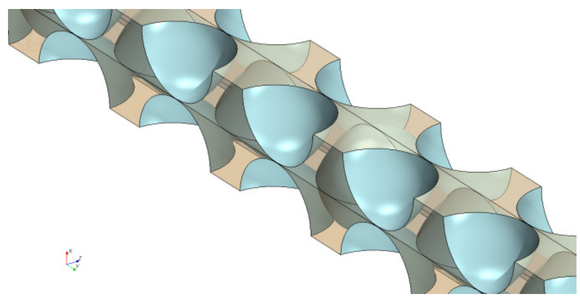

Figure 4 – Geometric Domain Developed for BCC Packed 1.5" Diameter Catalyst Spheres

Upon construction of the computational grid, the model is then analyzed using a range of superficial velocities within the expected operating limits. Figure 5 shows the flow streamlines from the model shown in Figure 4 for a superficial velocity of 1 m/s. For each of these cases, the calculated pressure drop per unit length is queried from the model. Once the data is known for at least three (3) superficial velocity conditions, the same curve fit procedures demonstrated with the Ergun-predicted pressure drops above can be used to develop the porous media parameters. Figure 6 shows such a fit performed for the 1.5" diameter particles, with equivalent data from a fit performed with Ergun-derived data. As can be seen, there is good agreement between the two (2) sets of data. It should be noted that due to limitations in the CAD software, the particles cannot touch at a single point; in this case a small interpenetration occurs between particles that reduces the void fraction to 40.5%.

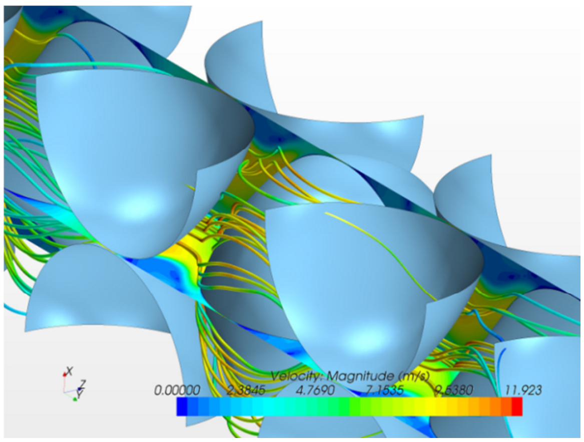

Figure 5 – Velocity Streamlines from Catalyst Particle Submodel

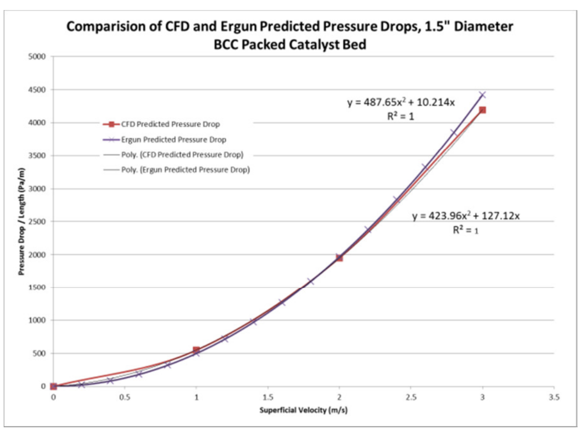

Figure 6 – CFD and Ergun Predicted Pressure Drops for BCC Catalyst Bed

3.3 Implementation of Porous Media within a CFD Model

Once the porous media coefficients have been determined, using either method described above or through test data, a CFD model can be constructed to solve for the quantities of interest. Construction of the model for this example starts with the geometry in Figure 1. From this geometry, five (5) fluid domains are be constructed (shown in Figure 7; colors are indicated in parentheses): upper gas space (cadmium lemon), 0.75" particle catalyst bed (orchid), 1.5" particle catalyst bed (lawn green), 2" particle catalyst bed (cornflower), and lower gas space (deep pink).

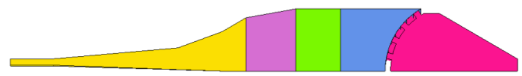

Figure 7 – Fluid Domains for Catalyst Bed Analysis

Notice from the figure that symmetry has been used to reduce the computational model size and that the refractory components shown in Figure 1 have been subtracted from the fluid domains. A computational grid is then constructed on the domains defined for the analysis. Next, appropriate boundary conditions are applied to the model and an iterative solution is conducted until the solution residuals have reached acceptable limits.

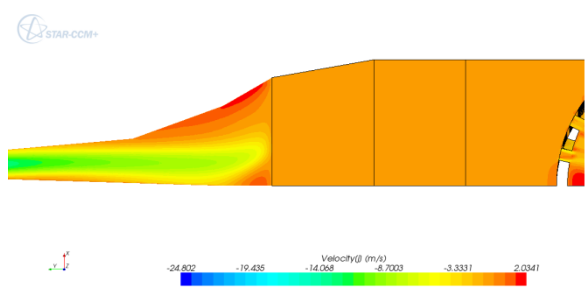

Figure 8 – Velocity Contours for Sample Expansion Chamber

3.4 Validation of Porous Media Models from CFD Analysis

After the solution residuals have reached acceptable limits, additional checks are performed to validate the model physics. In this case, one validation that should be performed is to compare the calculated pressure drop through each porous media domain to the expected values. The expected pressure drop in the 2" particle bed is difficult to estimate due to the bed's irregular geometry. Therefore, checks will only be performed on the 0.75" and 1.5" particle beds. Table 1 details the queried and expected values.

Table 1 – Queried and Calculated Values from Catalyst Bed Demonstration Model

Catalyst Particle Size (in)	Superficial Velocity (m/s)	Expected ΔP (Pa)	Calculated ΔP (Pa)	% Error
0.75	0.838	1534.37	1537.38	0.2
1.5	0.710	482.11	482.97	0.18

As can be seen from the table, good agreement is achieved between the expected pressure drops for both beds and the pressure drops calculated in the CFD model. In this case it can be concluded that the porous media approximations are exerting the proper back-pressure on the incoming flow due to the near bed velocity distributions. Therefore, it can be concluded that the calculated velocity distributions, as shown in Figure 8, are reasonable. The results indicate recirculation at the center and outside walls of the expansion chamber. As described in the initial problem statement, this violates one of the design goals. Additional analyses where the shape of the expansion chamber is modified to remove the recirculation would be required to meet the design goals.

4.0 Example 2 - TGU Optimization

As should be familiar to the audience, a primary design requirement for TGUs is that the pressure loss across the vessel should be low to minimize compression requirements. It should be intuitive that the flow into the catalyst bed should be as evenly distributed as possible and bed bypass should be avoided to optimize the use of the catalyst. In this example, a new world-class TGU was under design. There were two primary design variants, a variant with three (3) downcomers from the main pipe header and a variant with four (4) downcomers from the pipe header, as shown in Figure 9.

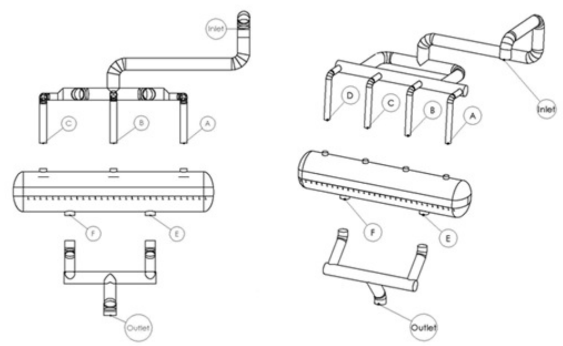

Figure 9 - TGU Variants under Consideration

Two primary goals were established at the start of the CFD analyses: a) to use CFD models of each variant to choose a candidate for final detailed design, and b) to use CFD to optimize the chosen variant during detailed design. During the optimization step, a goal was established to estimate the amount of bed bypass that was occurring in the near wall region. The procedures used to establish this value are demonstrated in Section 4.2, Final Design Optimization.

4.1 Selection of Design Candidate for Optimization

First, CFD models were developed of each variant with the primary goal of determining which inlet piping configuration would be a better candidate for the final design. Factors under consideration in selecting the final design candidate included: total system pressure drop, bed pressure drop, variance of flows through the downcomers and distribution of flows into the beds. To properly capture these phenomena required the inclusion of the influence of the bed on the total system flows.

As shown in Figure 10, for both vessel designs the catalyst consisted of a packed bed supported by W-shapes. An intermediate wire mesh was placed between the beams to support the catalyst particles in the spans between beams. Constant size catalyst particles were placed into the bed space and vibro-packed to produce a consistent particle void fraction. Finally, a second mesh was placed on the bed to provide capture of the catalyst particles.

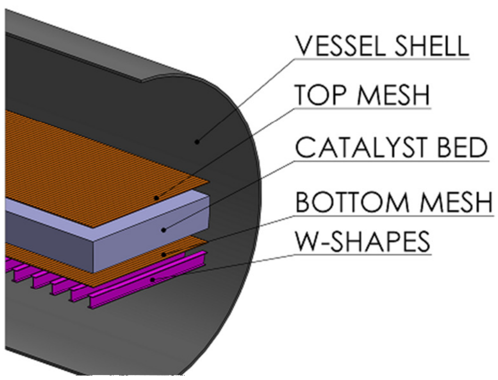

Figure 10 – Exploded View of TGU Catalyst Bed Layout

For the initial analysis of this design, it was decided to explicitly model the penetration of the support I-beams in the outlet fluid space and to model the bed using a porous media model. In these models, no consideration was given to the top and bottom mesh components as their fluid resistance was negligible compared to the bed's resistance. The Ergun equation was used to determine the porous media coefficients using the procedures described in Example 1. Steady-state analyses were performed on both models, and the design variables of consequence (described above) were queried from each model. Queried values for the total system pressure drop and for the pressure drops calculated across the catalyst beds were identical within accepted model uncertainties. Therefore, neither of the quantities provided specific insight into which design variant presented the best option for the final design.

To provide more insight into the performance of each design variant, the velocity magnitudes and distributions were surveyed from each model through the use of contour and streamline plots. Figure 11 shows the inlet velocity contours for each of the analyzed design variants. As can be seen from the contours, the three (3) inlet design displayed significant biasing towards the central downcomer. In this case approximately 20% more volume flow entered the vessel at this location than in the two (2) outboard downcomers. Also evident from the figure is that the flow in the four (4) downcomer design is well distributed between all downcomers, displaying less than 5% velocity (volume flow) variance between individual legs.

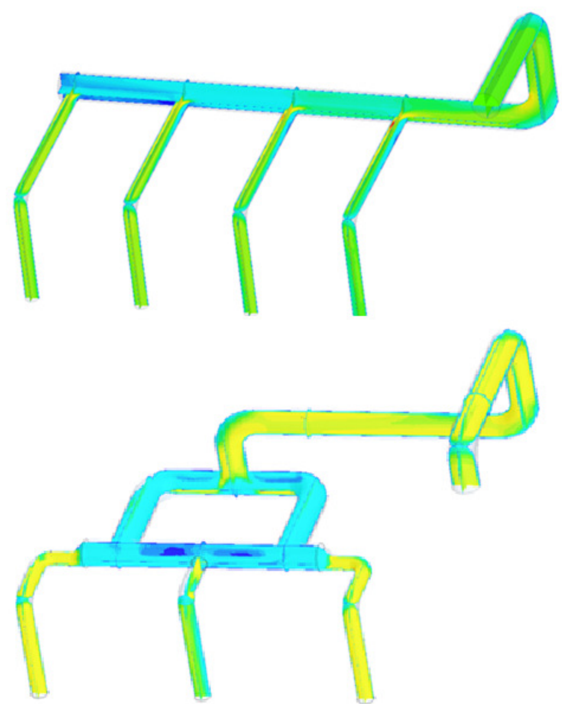

Figure 11 – TGU Inlet Piping Velocity

Next, the velocity distributions within each reactor were surveyed by using velocity contour and streamline plots. Figure 12 shows a sample of these plots.

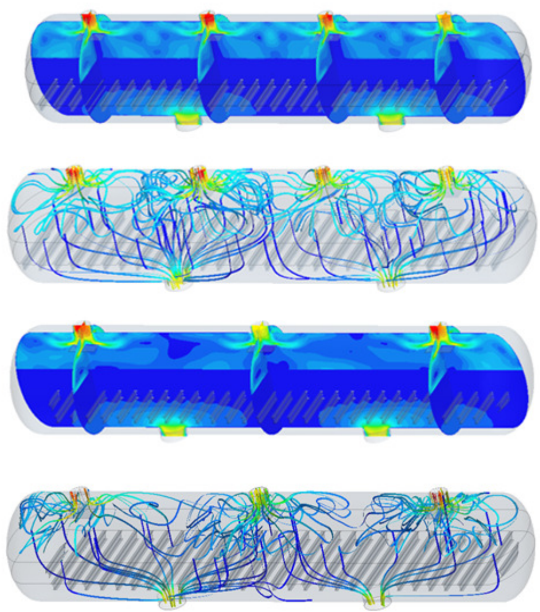

Figure 12 – Contours and Streamlines of Velocities inside the TGU Reactor, Initial Analysis

As can be seen from the figure, for both design variants, the flow enters the vessel and impinges on a deflector plate. This plate causes the flow to make an abrupt (approximately 90°) turn in the vessel. Once the flow turns, the portion directed towards the sides of the vessel flows unimpeded towards the catalyst bed along the curved walls of the vessel. The portion deflected along the axis of the vessel impinges either on the vessel's heads or on adjacent streams. These streams form recirculating vortices in the flow that limit a direct flow path to the catalyst bed. From visual inspection of the images in Figure 12, it can be concluded that the flow into the bed was likely not evenly distributed. To better estimate the maldistribution of the flow at the bed face, velocity maps were created for the vertical velocities directly above the bed. Figure 13 shows these vertical velocity maps. As can be seen from the figure, there is a strong biasing towards the periphery of the catalyst bed in both designs, with little to no downward vertical flow occurring in the center portion of the beds. This amount of flow biasing likely indicates that the majority of the catalyst bed is not being used in this flow configuration.

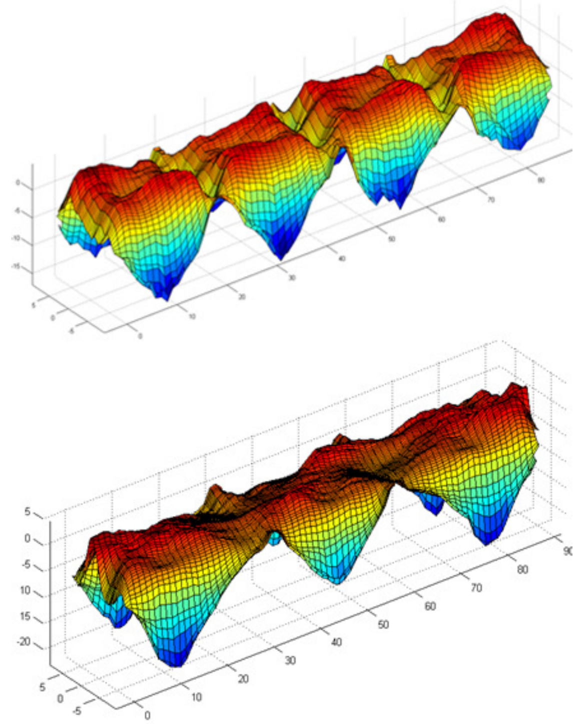

Figure 13 – Velocity Maps above the Catalyst Beds, Initial Analysis

Review of the results for both designs from the initial CFD analyses did not indicate a significant difference in operational pressure drops, but did indicate that the design with four (4) downcomers provided better volume flow distribution into the reactor. Additionally, both design variants demonstrated extreme flow biasing that occurred in the reactor vessel likely leading to non-optimal use of the catalyst in the bed. Most of the deciding factors between variants caused insignificant differences. Due to the more even flow distribution, it was decided to select the design with four (4) downcomers, for the final design.

4.2 Final Design Optimization

To support the final design effort, a series of analyses were performed with modified four (4) downcomer models, with the goals of: a) quantifying the level of bed bypass that occurred in the near wall vicinity, and b) minimizing the level of near wall bypass that occurs.

4.2.1 Quantifying Bed Bypass

Research published by Zong and Talbot [7] on bed packing in the near wall vicinity indicated that no matter the type of bed packing that was present - BCC from Example 1, face-centered cubic, Kepler's maximum packing density, etc. - there exists a region within four (4) and six (6) sphere diameters of the wall where the bulk packing fraction does not exist. This is due to the presence of the wall disturbing the regular ordered packing structure. The packing in this region can be considered to be random and chaotic, precluding prediction of the packing fraction using standard packing dynamics, although it can be shown that normal bed void fractions of 0.35 – 0.45 can rise to values approaching 0.8 – 1 at the wall [8]. A method of predicting a lower bound for the change in packing fraction is to modify the geometric model shown in Example 1 to not include the center packing sphere at the wall, as shown in Figure 14. For this condition the near-wall void fraction increases from 40.5% in the bulk region to 46.8% in the near wall region. While this change may seem negligible, when these packing fractions are inserted into the turbulent portion of the Ergun equation (Equation 8), the predicted inertial resistance is only 58.3% of the bulk value. As can be imagined, with more complex packing geometries, and as the void fraction approaches 1, the resistance the packed bed provides to the flow approaches zero.

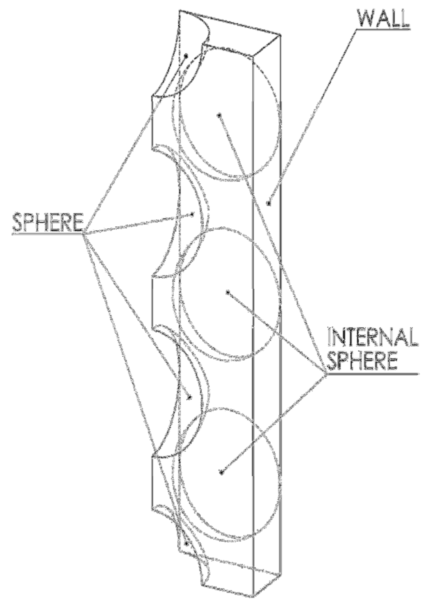

Figure 14 – BCC Cavity Model Modified to Account for Near Wall Packing

The same research indicates that the best approximation for the variance in void fraction and its corresponding change in porous resistance, is to use a series of exponential functions to describe the bed packing fraction in the near wall vicinity. While the use of exponential functions is convenient when modeling rectangular channels, or when considering theoretical packings within a larger sphere, the shape of beds within process vessels, especially as shown in this example, do not present regular walls that can be taken as flat. (In the rectangular case, a Cartesian coordinate system can be used; in a sphere, a spherical coordinate system can transform the wall to flat.) The lack of a flat wall makes introducing exponential functions to model the bed's packing fraction in the near wall vicinity difficult to implement in the CFD software.

To introduce the near wall change in void fraction and the corresponding reduction in flow resistance, it is convenient to introduce tortuosity, a concept first proposed by Bear and Bachmat [9]. Tortuosity is a measure of the length of a free path through a porous media (Le) versus a unit path length with no flow blockage (L), as shown in Figure 15, or "a dimensionless parameter that accounts for the fact that the flow path is generally not straight".

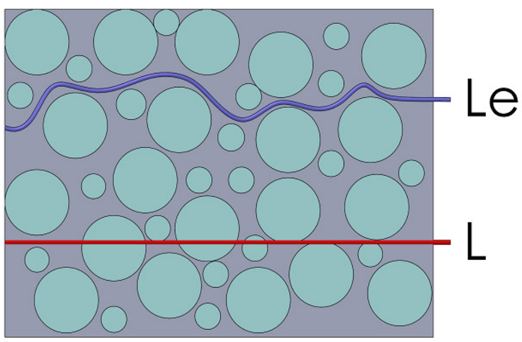

Figure 15 – Unit Path Length and Flow Path with Obstructions

Using the concept of tortuosity and with the knowledge that the bed void fraction will change in the near wall vicinity, Bear and Bachmat proposed that the flow domain can be considered to consist of two (2) regions, a near wall region and the bulk bed region, with each of the regions having its own tortuosity value. Further, they demonstrated that unless the flow characteristics at the interface between the regions with different tortuosity values were of critical importance that acceptable results could be obtained by implementing a step change in tortuosity for the near wall region without the use of exponential functions to modify the packing in the near wall region. As will now be shown, this methodology is very suitable for implementation in CFD models.

The following general steps are used to implement the near wall loss of packing fraction in CFD models.

1. As shown in Figure 16, the bed is separated into two (2) flow domains, a near wall domain (orange) and a bulk bed domain (lavender). Based on the work reported by Zong and Talbot, two (2) models were developed for analysis, a model where the transition to the domain with reduced tortuosity was four (4) particle diameters from the wall and a domain where the interface was six (6) particle diameters away from the wall.

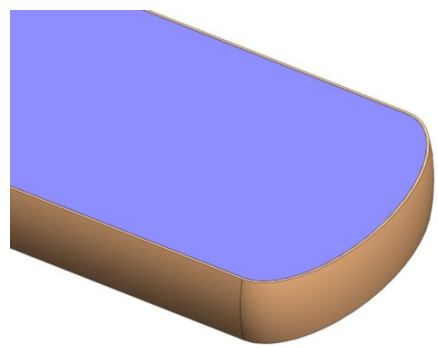

Figure 16 – TGU Catalyst Bed Domains for Consideration of Near Wall Tortuosity

2. The bulk bed's porous media parameters were developed using the Ergun equation with the bed's nominal packing fraction.
3. The porous media parameters for the near wall region were developed. In this case, a geometric model that assumed face-centered-cubic packing was developed and the void fraction was measured from the model. This void fraction was then used to develop the porous media constants using the Ergun equation. It should

be noted that other methods that include the use of CFD submodels, as described in Example 1, or using reduced packing fractions as reported by Yun, et. al. could be used [10].

With the modifications required to simulate the increased void fraction in the near wall region, the models were analyzed to estimate the expected amount of bed bypass. For both models, four (4) and six (6) diameter transition distance, it was found that approximately 300% more flow passed through the near wall region than would be expected due to geometry considerations. The fact that this value did not significantly change between models provided confirmation of both Zong's packing hypothesis and Bear's proposed methodology.

At this point in the optimization, the decision was made to explore design options that could reduce or eliminate bed bypass in the near wall region. Recall from Figure 12 that in the base design configurations, the flow entered the vessel and immediately impinged on a strike plate. This strike plate caused the flow to make an abrupt 90° turn where flow tangential to the vessel traveled down the shell wall and impinged on the side of the bed where reduced packing due to wall effects existed. It was concluded that the combination of the impingement and the reduced flow resistance in the near wall region was leading to the high rate of bed bypass. It was clear that if steps were taken with the design to reduce the velocity tangent to the vessel's shell, directing the velocities instead towards the center of the bed, that the amount of bed bypass should be reduced.

To accomplish this task, a series of submodels was used to design a custom diffuser structure for each vessel inlet with the goal of reducing the velocities directly impinging on the bed, while directing the flow toward the bed's center. Figure 17 shows the flow contours and streamlines for the vessel with the optimized inlet diffusers included. As can be seen from the figure, very little of the flow is directed tangentially to the shell, resulting in impingement on the bed sides where the reduced packing exists.

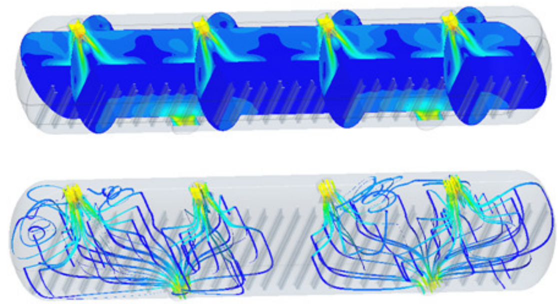

Figure 17 - Velocity Contours and Streamlines for TGU with Inlet Flow Diffusers

Figure 18 shows the velocity map queried from the model directly above the bed. It is also evident from this figure that the areas of high velocities at the bed location have been redirected from the side of the bed to the center. In this case the CFD model indicated that the amount of bed bypass that should occur with the optimized design would be reduced by approximately 50% from the original design, a substantial increase in the use of the catalyst. This level of reduction in bed bypass was considered to be adequate for the design, although the CFD model provided other indications where additional design steps may be taken to further reduce bypass.

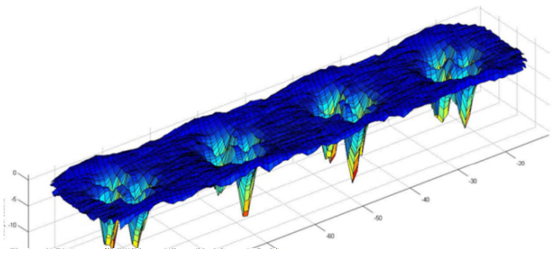

Figure 18 – Velocity Map for TGU with Optimized Inlet Diffusers

Figure 19 shows the vertical velocities through the bed at three (3) cut plane depths.

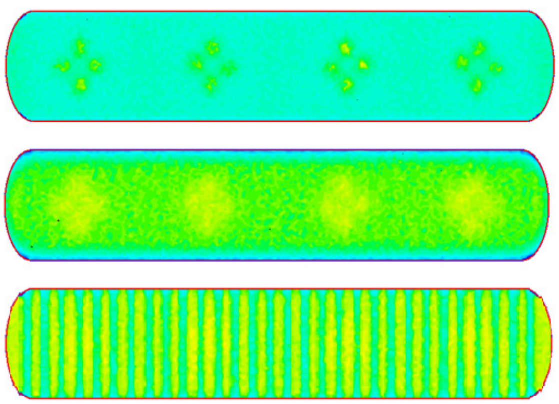

Figure 19 – Vertical Velocities through Catalyst Bed (¼, ½ and ¾ Depth)

Two (2) flow features are evident in the bed from this plot:

1. High vertical velocities exist throughout the bed's depth in the near wall region. This indicates that once flow enters the region of reduced packing, there is a high probability that it will bypass the bed. This is intuitive from a flow dynamics standpoint, because in the reduced packing region there is a reduced driving force to turn the flow into the bulk bed region.
2. As shown in the lowest image in Figure 19, the flow must accelerate at the bottom of the bed due to the w-shape cross supports and the reduced open area at this location. The acceleration of the flow will cause two (2) primary effects that should be considered during design. First, the contact time between the catalyst particles and the process gas stream will be reduced. In extreme cases, it may be reduced enough to affect the efficiency of the vessel. Second, as shown in Equations 6 and 7, the pressure drop through the bed will be dependent on the superficial velocity. Therefore, the increased velocities caused by the support structure will result in a higher pressure drop through the bed. Both of these factors should be considered during design.

It should be noted that the modifications to the TGU were implemented in the final design and that the design has successfully operated for five (5) years without requiring new catalyst. Using targeted CFD analyses, a final design candidate was selected that only displayed a variance of +/- 2% in flow rates at the vessel nozzles, versus the +8%, -17% that occurred with the three inlet design. Before the diffuser optimization analysis, the standard deviation of velocities above the bed was 4.5 ft/s. After the optimization analysis, the standard deviation was 2.4 ft/s, a reduction of 47%.

5.0 Example 3 – Amine Carbon Filter Bed

An amine carbon filter bed, shown in Figure 20, was under detail design. It was desired to determine if there was any advantage to placing the inlet nozzle in the top or side of the vessel's head. Additionally, it was hypothesized that a previous design experienced bed bypass during operation. Therefore, a second goal was established, to determine the propensity for the flow to bypass the bed and the level of bed bypassing that could occur. A final goal of the analysis was to determine the effect on the bed's performance that could be caused by voids or inclusions.

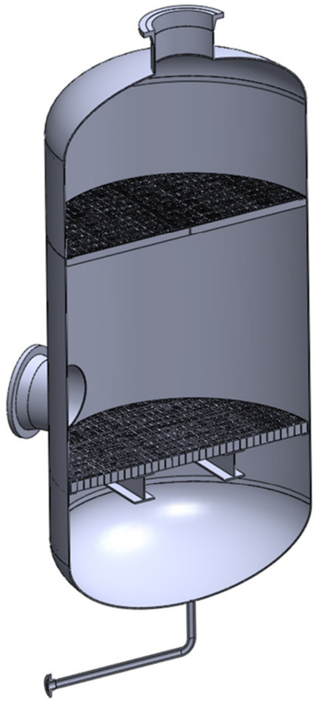

Figure 20 – Amine Carbon Filter Bed

As can be seen from the figure, the vessel has two grates that function very similarly to the grates described in Example 2. In this case the bottom support grate is supported by two (2) w-shapes and the top grate provides catalyst particle capture at the top of the bed. In Figure 20, a center support bar is visible for the top grate, whereas in reality it is thin, Unlike Example 2, the bottom support grate is classified as thick, thus requiring its inclusion in the CFD model. As was the case with Example 2, the w-shapes were explicitly modeled. To capture the near wall bypass that could be expected to occur, the bed space was modified, as shown in Example 2, to include the near wall change in packing fraction. In this case, only one model was developed with the interface at five (5) particle diameters from the wall. In the authors' past experience, and as shown in Example 2, there is very little difference in the four (4) and six (6) diameter results.

For this example, procedures will be demonstrated that show:

1. Determining orthotropic porous media constants for non-symmetric geometries
2. Constructing and analyzing the baseline CFD model, including the use of species tracer tracking, and
3. Modifying the bed geometry and porous properties to model inclusions or voids.

5.1 Determination of Grate Porous Media Properties

Figure 21 shows the geometry of the bottom support grate. As can be seen from the figure, the grate is not symmetric, having a long opening and short opening. While the flow resistance of many grate and screen-type structures have been published, for grate structures the flow is typically assumed to be along the opening, i.e., no cross-flow is considered [11]. It should be obvious that cross-flow through the long portion of the grate should offer less resistance than cross-flow through the short portion of the grate. Therefore, a methodology is needed to develop directional (orthotropic) porous model coefficients, rather than the isotropic properties that have been developed in Examples 1 and 2.

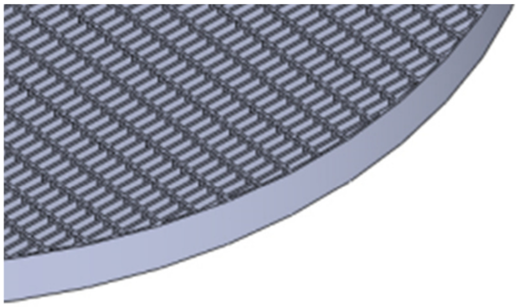

Figure 21 – Bottom Support Grate Geometry

Since little or no published data is available on the resistance characteristics of grates in cross-flow, a methodology is needed to derive the directional coefficients. It should now be understood, based on the information presented in this paper, that two methods are available to develop this data, physical testing or numerical modeling. For this example a CFD submodel will be developed, in this case a periodic submodel. A periodic model is similar to a symmetric model, where only a portion of the grate is modeled. In this case, one grate crossing and one-quarter (¼) of the flow space on each side of the grate crossing, as shown in Figure 22.

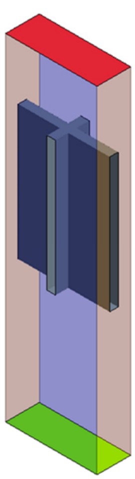

Figure 22 - Periodic Grate Model

Instead of applying symmetry boundary conditions on the side model boundaries (blue and peach in Figure 22), as shown in Example 1, periodic boundary conditions are applied at the model extents. The periodic boundary conditions transfer the flow information, such as pressures, velocities and turbulence quantities, from one set of periodic faces to the second set of periodic faces. Instead of only performing analyses with the flow normal to obstructions, as shown in Example 1, three (3) sets of analyses are performed: normal to obstruction, at an incident angle to the first direction of the flow obstruction, and at an incident angle to the second direction of the flow obstruction. At least three (3) superficial velocities are run for each of the cases, and the pressure drop is queried from the model. Figure 23 shows the velocity contours for one analysis performed at a 45° angle to the short flow path. Once the complete set of analyses has been performed, the following steps are taken to determine the porous media coefficients in each direction.

1. Perform the curve fit analysis to determine the porous media coefficients for flows normal to the obstruction.
2. Correct both oblique flow pressure drops for the flow normal to the obstruction, i.e., determine the expected pressure drop for the flow normal to the obstruction using the normal velocity and the curve fit performed in Step 1 and subtract it from the total pressure loss for each directional analysis.
3. Perform a curve fit analysis on the modified data from Step 2 to

determine the directional curve fit constants.

Figure 24 shows a sample set of curves developed using this technique. It should be apparent that this technique allows the analysis of any obstruction shape (beds, grates, etc.).

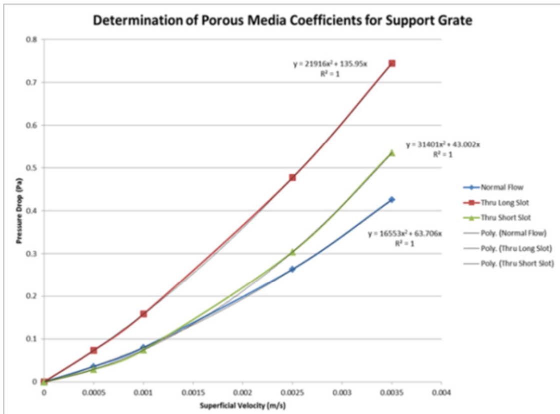

Figure 23 - Orthotropic Curve Fit Properties

5.2 Analysis of Baseline Model

As shown in Figure 25, the pressure drop versus flow rate was supplied by the carbon filter supplier. Instead of a second order fit, a linear fit can be used to find the porous media constant. It is apparent from the figure that only the viscous (Ergun laminar) term is expected to be active in the bed.

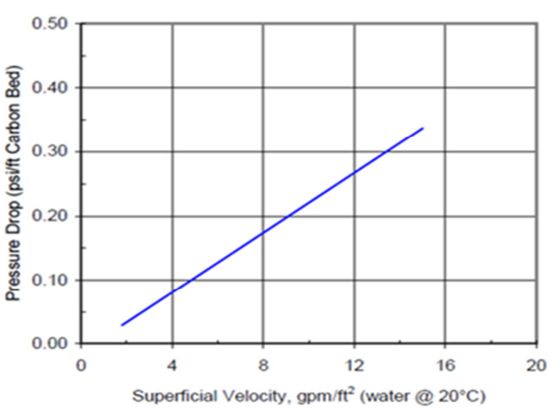

Figure 24 – Supplier Provided Pressure Drop vs. Flow Rate Curve

Once the bed input properties have been determined, the geometric model can be sectioned into the appropriate domains for analysis. Figure 26 shows a subset of the domains selected for the analysis model: upper open inlet volume (green), reduced packing fraction in the near wall (purple) and main bed packing (goldenrod). Not shown in the figure are the lower support grate domain and the outlet open volume domain.

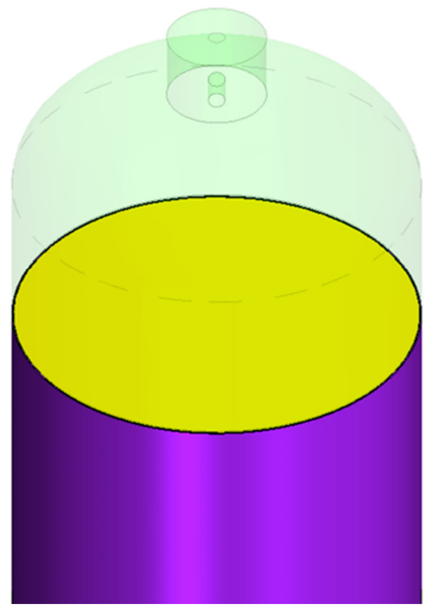

Figure 25 - Domains Used for Baseline Amine Bed Analysis

Curve fit properties, as derived in Section 5.1, were applied to the lower support grate. Properties based on the linear fit described above were applied to the main bed, and it was assumed a 10% loss in packing fraction near the wall (33% of original bed viscous resistance via Ergun). Three (3) analysis cases were run for each inlet condition, design flow rate, 90% of design and 130% of design.

Originally, the velocity contours on cut planes throughout the vessel were compared to determine if any differences in flow patterns were evident between inlet configurations. While some differences could be seen in the upper open inlet volume (as can be seen in Figure 27), the velocities in the bed section (on the order of a few inches per second) were too low to allow visual estimation of the differences between the flow patterns either between inlet configurations, or if additional bypassing was occurring at the higher flow rates.

Figure 26 - Sample Velocities on Cut Planes through the Vessel

For this reason, it was decided to perform statistical analyses on the velocities within the bed for each analysis. The primary statistical tool chosen for this analysis was the cumulative distribution function (CDF). CDFs provide a numerical and graphical method to determine the probability that a given variable will be at or below a value; in this case, the probability (in volume %) that the velocity is at or below a certain value. Figure 28 shows the distribution functions for the six (6) analyses described above. A "perfect" CDF will be a vertical line at the nominal value. As can be seen from the figure, all cases performed almost perfectly and the difference between each model could be considered solution uncertainty. For this reason a second method, tracer washout testing, was used to quantify the performance of the models.

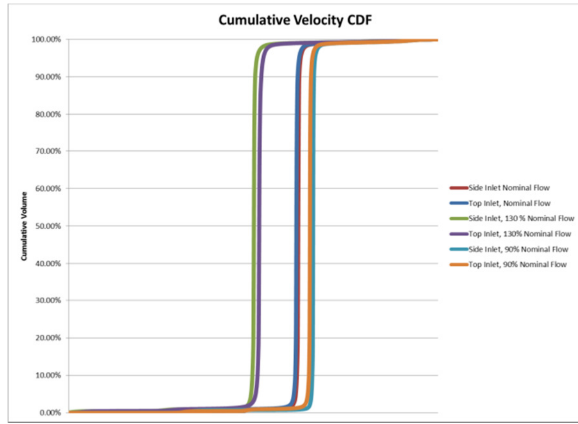

Figure 27 – CDFs for Baseline Analysis

5.2.1 Tracer Washout Testing

Species tracking with CFD provides a particularly valuable tool to track how substances move through the flow medium, other than normal flow visualization options. In the CFD case, a second species having the exact physical properties of the working fluid, is injected starting at a certain time during a transient analysis. The mass or volume fraction of this species is then tracked at locations downstream and the tracked fractions can be compared to the theoretically perfect case to determine the amount of bypassing that is occurring and the amount of flow that becomes entrained, long-term, in stationary eddies.

The following common steps were used in this case:

1. A base species $amine_a$ was defined to fill the entire solution domain
2. t time t=0 a second species, with the same properties, $amine_b$ was injected for a period of 100 seconds at the inlet
3. Monitors were established on the top and bottom of the bed to measure the

species volume fraction at each time-step, as shown in Figure 29

4. The product of the mass fraction and volume flow was used to compute the flow of the species on each surface for each time-step
5. This product was integrated to find the total amount of species that had passed through the surface at a given time-step
6. The outlet curve is transformed in time by the theoretical bed residence time (bed depth/average bed through velocity)

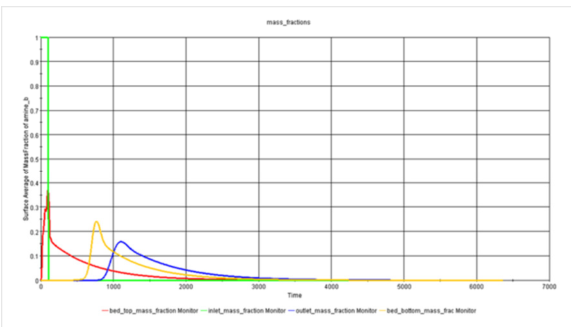

Figure 28 – Sample Species Volume Fraction Tracking Plot

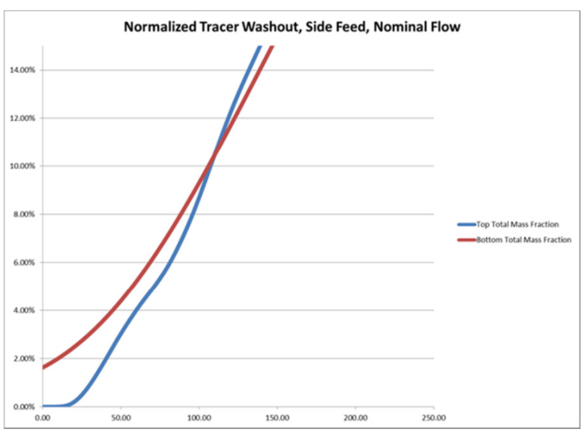

Figure 29 – Sample Tracer Washout Curve

Of particular interest is the behavior of these two curves near the injection time (accounting for the time transformation at the outlet location). Figure 30 shows a sample washout curve. On this graph the species mass fraction at the top of the bed is shown in blue and the species mass fraction at the bottom of the bed is shown in red. There are two points of particular interest on the chart: a) the value of the percent washout on the bottom of the bed at time zero, this indicates the amount of flow that has "short-circuited" the bed, and b) the point where the curves cross, which represents the total mass fraction of the flow that does not achieve theoretical retention time. On this plot, the values are approximately 2% total bypass and 10% less than theoretical retention time. In general these values indicate good performance of the bed, while these bypass values are much higher than the theoretical values based on the open area in the near wall region. The total magnitudes are not that great and the reduced contact time due to bypass is on the order of 50 seconds. There are other integrals that can be performed to provide additional quantification of the beds performance, but they are outside of the scope of this paper.

As can be seen from the example presented above, the use of tracer tests provides a framework to quantify, within the limits of model uncertainties, the exact performance of a catalyst bed.

5.3 Determination of the Effects of Inclusions or Voids

The final goal of the analyses was to quantify the additional amount of bed bypass that could occur due to interstitial voids or cracks. It should be apparent that it is not possible to characterize the geometry of a void in the center of a bed during operation. For this it was chosen to modify the baseline model to characterize an increase in porosity in 5%, 7.5% and 10% of the total bed volume. This type of characterization would allow a bracketing analysis where it could be determined if large amounts of bypass could be caused by a relatively minor void, and/or if there was a point where a "fall-off-the-cliff" type event occurred where the amount of bypass occurring increased considerably for the increase in bed void. To perform this analysis the main bed model (shown in Figure 26) was modified with three (3) additional volumes to represent the loss of void, as shown in Figure 31 (grey 5% void, grey + blue 7.5% void, and grey + blue + red 10% void).

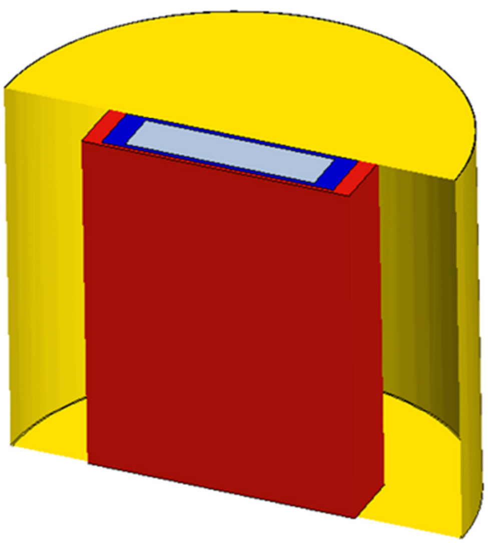

Figure 30 – Modified Bed Model

Tracer washout tests were performed at design flow rate and one inlet configuration and the results were compared using both velocity CDFs and cumulative tracer tests, as shown in Figures 32 and 33, respectively. From these figures it can be seen that there is some increase in volume of the bed that exists at velocities higher than the bulk bed velocity, and there is a slight increase in the amount of tracer that passes through the bed in less than the theoretical time. Both results were expected.

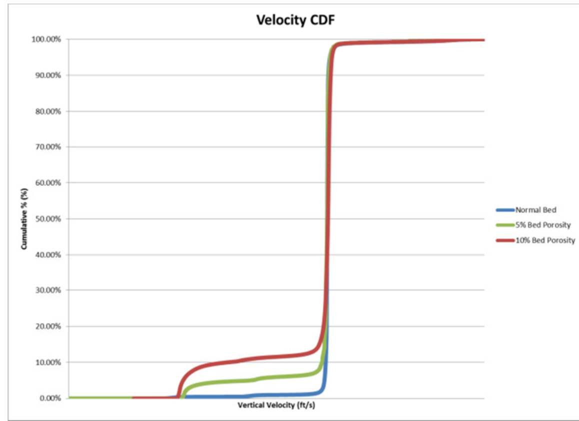

Figure 31 - Velocity CDF with Bed Voids

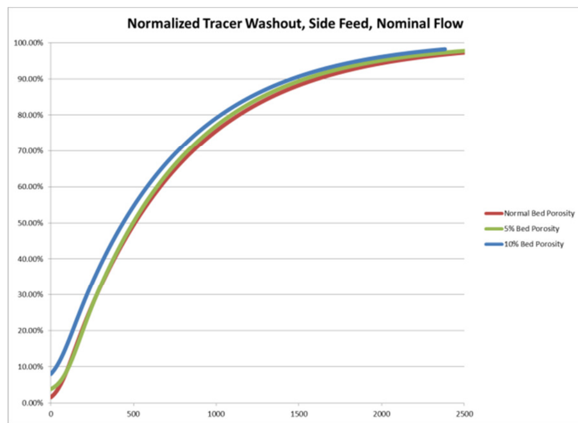

Figure 32 - Tracer Washout with Bed Voids

Comments and Conclusions:

Packed beds are critical in sulfur recovery equipment such as condensers, converters, tail gas units and amine filters. To optimize process conditions, it is necessary to make the most efficient use of beds to ensure that adequate contact time is maintained and that the amount of bed bypass is minimized. To meet these criteria the flow upstream and through the bed must be optimized. The two methods of optimizing the flow are to use physical flow models or CFD models.

Physical flow models have limitations that include cost, lack of similitude and limitations in visualization of flow patterns. CFD models avoid problems with similitude in a framework that provides better flow visualization options than can be achieved with physical testing. While CFD has a reputation for being costly (due to being very computer intensive) and requiring highly specialized individuals to conduct the modeling, recent advances have made moderate sized models "affordable". Due to the number of particles in beds (millions) and the requirements for constructing models with geometric fidelity, it is not feasible to model the exact dynamics of the flow within beds with moderate sized models. For this reason the microscopic details of flows through the beds' catalyst particles are typically not modeled. Instead, the bed is replaced by a porous media. Within a CFD model the porous media approximation behaves as a momentum sink by imposing a pressure drop as a function of the superficial velocity that the medium is exposed to.

As shown in this paper:

- The coefficients that control the pressure drop through the medium can be readily determined through physical testing, by using empirical relations or through the use of CFD submodels
- In addition to modeling the porous media as a single bulk component, it is also possible to modify the porous media model to account for a reduction in packing fraction (increase in void fraction) in the near wall region. These model modifications allow much better prediction of the level of bed bypass that occurs in the reduced resistance volume.
- Coefficients can be developed using submodels to allow the consideration of not only packed beds, but also grate and tray type structures.
- With CFD it is possible to conduct multi-species tracer analyses to quantify the amount of bed bypass along with the impact on residence time within the bed.

It should be noted that the analyses presented in this paper, performed by qualified individuals, can be classified as routine analyses that can be incorporated into any process equipment design cycle. The authors' goal in preparing this paper is that the reader understands the level of flow detail that can be extracted from CFD models, both in terms of "pretty pictures" and hard numerical data, and how this data can be used to streamline and improve the flow characteristics of process equipment.

REFERENCES

[1] Munson, B.R., Young, D.F., Okiishi, T.H., Fundamentals of Fluid Mechanics, Second Edition, John Wiley & Sons, Inc., 1994

[2] Star-CCM+ v. 8 Users Guide

[3] ANSYS FLUENT 12.0 Users Guide

[4] CFX 12.1 Solver Theory Guide

[5] Rostrup-Nielsen, J., and Christiansen, L.J., Concepts in Syngas Manufacture, Imperial College Press, 2011

[6] Ergun, S., Chemical Process Engineering, London 48, 1952

[7] Zong, C., and Talbot, J., Sphere Packings, Springer, 1999

[8] Cheng, P., HSU, C.T., Fully-developed, forced convective flow through an annular packed-sphere bed with wall effects, International Journal of Heat and Mass Transfer, 29, 1986

[9] Bear, J., Bachmat, Y., Introduction to Modeling of Transport Phenomena in Porous Media, Kluwer Academic Publishers, 1991

[10] Yun, M., Yu, B., Xu, P., Wu, J., *Geometrical Models for Tortuosity of Streamlines in Three-dimensional Porous Media*, Canadian Journal of Chemical Engineering, 2006

[11] Idelchik, I.E., Fried, E., Handbook of Hydraulic Resistance, Second Edition, 1986

Appendix – A, THEORY:

The following sections contain the theoretical basis for discussions in the paper. There are three (3) primary categories, listed below with their relevant sections.

- Theory of similitude with dimensional analysis (Introduction)
- Implementation of porous media models in common CFD solvers (Porous Media, the Basis), and
- The Ergun equation (Example 1 – Multi-layer Catalyst Bed)

A.1 Theory of Similitude with Dimensional Analysis

From Buckingham in the basic theorem of dimensional analysis, dimensionless variables are known as Π terms. It is the goal of basic fluid analysis to describe one dimensionless parameter as a function of other dimensionless terms, or:

$$\Pi_1 = \phi(\Pi_2, \Pi_3, \Pi_{etc\ldots}) \tag{1}$$

The theory of models states that for the model's functional term (indicated by subscript m), Π_{m1}, to predict the system's functional term, Π_1, that the model's variable terms, Π_{m2}, $\Pi_{metc.}$, must be equal to the system's variable terms, Π_2, $\Pi_{etc.}$.

Let's examine this in slightly less esoteric terms. Consider the drag on a flat plate exposed to flow. It is known that the drag force on the plate ($\mathfrak{D}$) will be a function of the plate's width (w), height (h), the fluid's viscosity (μ), the fluid's density (ρ), and the velocity over the plate (V), or:

$$\mathfrak{D} = f(w, h, \mu, \rho, V) \tag{2}$$

Application of dimensional analysis produces:

$$\frac{\mathfrak{D}}{w^2 \rho V^2} = \varphi\left(\frac{w}{h}, \frac{\rho V w}{\mu}\right) \tag{3}$$

From the theory of models it can be stated:

$$\frac{\mathfrak{D}_m}{{w_m}^2 \rho_m {V_m}^2} = \varphi\left(\frac{w_m}{h_m}, \frac{\rho_m V_m w_m}{\mu_m}\right) \tag{4}$$

Therefore, for the models to be similar the following conditions must be met:

$$\frac{w_m}{h_m} = \frac{w}{h} \qquad \frac{\rho_m V_m w_m}{\mu_m} = \frac{\rho V w}{\mu} \tag{5}$$

A.2 Implementation of Porous Media Models in Common CFD Solvers

Mathematically, ANSYS-FLUENT and ANSYS-CFX both describe the loss through a porous media using the following formulation (note variable call-outs will change between manuals) [3, 4].

$$S_i = -\left(\frac{\mu}{\alpha} v_i + \frac{1}{2} C_2 \rho v_i |v|\right) \tag{6}$$

Where:
S_i – Directional sink term
μ – Dynamic viscosity
α - Permeability
v_i – Directional velocity
C_2 – Inertial resistance factor
ρ – Density
$|v|$ – Velocity magnitude
Star-CCM+ uses a slightly different formulation for the sink term:

$$\frac{\Delta P}{L} = -(P_i|v| + P_v)v \tag{7}$$

Where:
ΔP – Pressure loss
L - Mean path through region (bed depth)
P_i – Inertial resistance coefficient
P_v – Viscous resistance coefficient
v – velocity

A.3 The Ergun Equation

$$\frac{\Delta P}{L} = \frac{150 \mu v_s L}{D_p^2} \frac{(1-\varepsilon)^2}{\varepsilon^3} + \frac{1.75 L \rho v_s^2}{D_p} \frac{1-\varepsilon}{\varepsilon^3} \tag{8}$$

Where:
ΔP – Pressure drop
L – Bed depth
μ – Fluid dynamic viscosity
v_s – Fluid superficial velocity
D_p – Diameter of particles
ε – Bed void fraction